Diffraction of He Atoms at a Si(111) 7 × 7 Surface

M. J. Cardillo and G. E. Becker
Bell Laboratories, Murray Hill, New Jersey 07974
(Received 1 November 1978)

We report the diffraction of He atoms at the Si(111) 7×7 reconstructed surface. The atom diffraction patterns consist of numerous sharp peaks filling out the seventh-order net observed by low-energy electron diffraction (LEED). In contrast to low-energy electron diffraction, the diffraction intensities in this seventh-order net are determined by only the outermost exposed layer of silicon atoms. These results should be sufficient to allow a semiclassical scattering calculation to test critically the various structural models which have been proposed for this reconstruction.

We report the diffraction of a thermal-energy He beam from the (7×7) reconstructed face of the Si(111) crystal. The atomic diffraction shows a sharp and complete seventh-order array of peaks whose intensities vary with incident angle and wavelength. The diffraction peaks extend to large values of parallel momentum transfer, $\Delta k_{\parallel} = (2\pi/\lambda)(\sin\theta_r - \sin\theta_i)$, with as many as 22 peaks of rapidly varying intensity occurring in one angular scan in the plane of the incident beam and surface normal. Since the He atoms are completely nonpenetrating, these seventh-order diffraction intensities result from the periodic structure of the outermost exposed atomic layer.

The reconstruction of the Si(111) surface to form a 7×7 unit mesh has been known for nineteen years[1] and has been the subject of numerous structural investigations since.[2] To data no convincing evidence to support any of the structural models proposed has emerged. In part this is due to the large size and complexity of the unit mesh. In addition, low-energy electron diffraction (LEED), which is the most common probe of surface structures, samples to a depth exceeding 10 Å, thereby making a structural determination of the outermost layer of a reconstructed surface most difficult. On the other hand, it is becoming apparent that another diffraction process, namely diffraction of light atoms from crystal surfaces, may often be more appropriate for the determination of the surface geometries. Although the experiment is not as easily performed as LEED, atomic diffraction patterns are extremely sensitive to the shape of the unit mesh potential and, at the energies employed (10–200 meV), the scattering process is completely restricted to the outermost exposed layer of atoms. For Si(111) this is probably the top double layer. The absence of attenuated multiple scattering from the bulk or selvedge allows fairly rigorous calculation of the atomic diffraction patterns for a given structural model. We think that the diffraction spectra reported here are sufficient to test critically each of the geometric models so far proposed for the reconstruction of the outermost exposed layer of the (111) 7×7 surface of silicon.

The apparatus employed has been described elsewhere.[3] It consists basically of a nozzle molecular beam source which produces a He jet of narrow velocity distribution, a beam modulation chamber in which the beam is collimated to 0.06°, and an ultrahigh-vacuum scattering chamber ($P = 1.5\times10^{-10}$ Torr). The latter contains a differentially pumped quadrupole mass spectrometer which rotates in the plane of the beam and surface normal, an Auger electron spectrometer (AES), and separate LEED optics. The experiments were run in a manner similar to our previous diffraction study of the Si(100) surface.[4] The only significant change was an improvement in resolution. The mass-spectrometer acceptance angle was reduced from 1.4° to 0.56°, and most diffraction data were obtained for a He-beam expansion from a cooled nozzle source ($T_N \simeq 95$ K), with a wavelength of 1.0 Å and a normalized full width at half maximum (FWHM) of 4.2%. Some data are reported for room-temperature nozzle expansions which give a wavelength of 0.57 Å and a FWHM of 10–12%.

The crystal was cut and polished outside the vacuum chamber and cleaned *in situ* by ion bombardment. It was then annealed at 1150°C for 2 min and slowly cooled to room temperature (~3°/sec). This procedure produces a sharp 7×7 LEED pattern, an AES spectrum with carbon as the sole residual impurity [peak-to-peak ratio of C(272 eV) to Si(92 eV) of 0.001], and sharp atom diffraction peaks. We note that with Ar^+ bombardment followed by a 10-min anneal at 800°C we were able to reduce the C/Si AES ratio to only 0.007. However, a check of the atomic diffraction spectrum at $\theta_i = 75°$, $\lambda = 0.57$ Å showed no significant differences for the two types of surface preparation.

In Fig. 1 we show diffraction scans in the $[0\bar{1}]^*$ direction for an incident angle $\theta_i = 70°$ at $\lambda = 0.57$ Å ($\bar{E} = 63$ meV) and $\lambda = 1.0$ Å ($\bar{E} = 20$ meV). The arrows show the expected peak positions for the 7×7 reconstruction. The agreement is excellent except for the peaks at grazing emergence in each case. This shift is qualitatively accounted for by the spread of the 1-mm incident beam across the crystal at $\theta_i = 70°$ and the extended area of the crystal viewed by the mass spectrometer at $\theta_r \simeq 80°$. The diffraction peaks are of intensity similar to that observed for the Si(100) surface[4] whereas the "background" is reduced as expected for the higher angular resolution of the detector. The widths of the peaks are accounted for by the wavelength distribution in the beam and the angular resolution of the detector. The total in-plane diffracted intensities amount to somewhat less than 1% of the incident beam I_0. The total number of diffraction beams allowed in and out of the detector plane, however, is very large ($\sim 10^3$) and there is some indication that the out-of-plane intensities in the vicinity of the intense in-plane peaks are considerable (see below and Fig. 2). Thus the total diffracted intensity may be a considerable fraction of I_0 consistent with the value of 10–20% suggested by the Debye-Waller factor.[5] With the azimuth rotated 60° we obtain a diffraction pattern qualitatively equivalent to that of Fig. 1.

In Fig. 2 we plot the diffraction pattern for a scan in the $[1\bar{2}]^*$ direction ($\varphi = 30°$) for $\theta_i = 60°$, $\lambda = 1.0$ and 0.57 Å. In Fig. 2(a) the detector acceptance angle, $\Delta\theta_r$ (for a point source on the crystal), is 0.56°, and the FWHM wavelength spread about $\lambda = 1.0$ Å is 4.2%. In Fig. 2(b) we plot the intensities obtained for $\lambda = 0.57$ Å ($\Delta\lambda/\lambda = 12\%$), $\Delta\theta_r = 1.4°$. The reciprocal net spacings for the 7×7 reconstruction are sufficiently small with respect to the incident-momentum wave vector ($|k_i \sim 11$ Å^{-1}, $d^* = 0.27$ Å^{-1}) that this $\Delta\theta_r$ is insufficient to eliminate the nearest out-of-plane peaks from the in-plane scan. Thus in Fig. 2(b) we see intense "extra" peaks of apparent fourteenth order appearing in between the expected seventh-order peaks in addition to a higher "background" level. Indeed, for this detector resolution at $\theta_i = 75°$ and $\lambda = 0.57$ Å, scans taken at $\varphi = 0°$–30° in 10° intervals reveal numerous "extra" peaks. With $\Delta\theta_r$ improved to 0.56°, scans in θ_r at $\theta_i = 70°$ for a series of φ at 10° intervals are

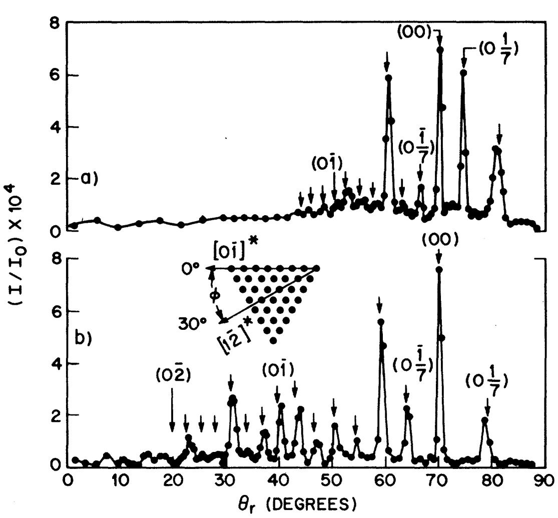

FIG. 1. Normalized scattered helium intensity for $\theta_i = 70°$, $\varphi = 0°$ vs scattering angle for (a) $\lambda = 0.57$ Å and (b) $\lambda = 1.0$ Å. The angular positions marked with arrows were calculated from the grating formula $n\lambda = d(\sin\theta_r - \sin\theta_i)$ with $d = 3.326$ Å ($n = 0, \pm\frac{1}{7}, \ldots$). The detector acceptance angle ($\Delta\theta_r$) is 0.56° for both plots. The wavelength dispersion (see text) is 10% for (a) and 4.2% for (b). The inset shows the reciprocal net for the (111) 7×7 surface with the convention we use for the azimuthal angle φ.

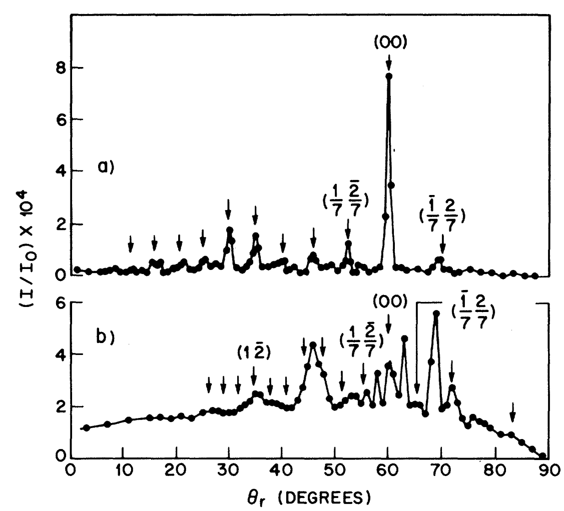

FIG. 2. Normalized scattered helium intensity for $\theta_i = 60°$, $\varphi = 30°$ vs scattering angle for (a) $\lambda = 1.0$ Å and (b) $\lambda = 0.57$ Å. The arrow positions were calculated using $d = 1.92$ Å in the grating formula. For (a), $\Delta\lambda/\lambda = 4.2\%$ and $\Delta\theta_r$ is 0.56°. For (b), the corresponding parameters are ±12% and 1.45°. The extra peaks in (b) are from the closest out-of-plane beams which are detected because of the greater angular acceptance range.

devoid of these "extra" features. Thus in Fig. 2(a), we note the absence of the extra features seen in Fig. 2(b) which are understood to be the nearest out-of-plane peaks to the in-plane scan. This figure gives an indication of the significant diffraction intensities scattered into the vicinal out-of-plane peaks for this surface.

In Fig. 3 we present a summary plot of diffraction intensities in the $[0\bar{1}]^*$ direction for four incident angles, $\theta_i = 70°$, $60°$, $45°$, and $30°$, at $\lambda = 1.0$ Å. The reduced intensities are plotted against $\Delta K_{\parallel}$ so that the alignment of the diffraction features can be observed. Note that the majority of data points correspond to increments in θ_r of 0.5°. There is some slight misalignment of the peaks which in part may be attributable to a wavelength shift during the experiment of ~1% due to a corresponding temperature change in the source of 2°C. Each scan is rich in diffraction features which extend well beyond the first integral peaks in both directions. We note that the *envelope* of the diffraction intensities in these scans is directly connected to the structure of the unit mesh.

The He-Si potential is primarily repulsive and

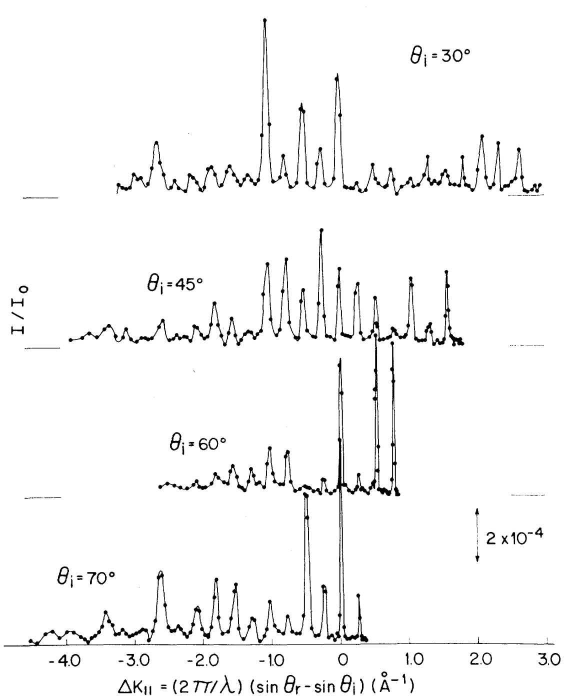

FIG. 3. Normalized scattered helium intensity vs parallel momentum transfer for scans in the $[0\bar{1}]^*$ ($\varphi = 0°$) direction, for $\lambda = 1.0$ Å. The grating relation allows diffraction peaks at multiples of 0.27 Å^{-1}.

one may examine these data qualitatively by considering classical specular scattering by a hard repulsive wall whose shape over the unit mesh is directly related to the atomic positions. This "shape function" in classical scattering predicts a continuous distribution of scattered intensity, independent of velocity, with rainbow maxima corresponding to each point of inflection in the shape function. In a more realistic semiclassical hard-wall calculation, although scattering appears only at the angular positions corresponding to the two-dimensional grating relation, the envelope of diffraction peak intensities is similar to the classical envelope. Additional modifications of the potential such as adding a long-range weak attraction and using a softer repulsion cause further (often minor) changes in the diffraction intensities and their angle and energy dependence. An illustration of the applicability of a hard-wall type of potential can be seen in Figs. 1(a) and 1(b). The spacings of the diffraction peaks are quite different yet the envelopes of the diffraction intensity maxima in scattering angle are remarkably similar for $45° < \theta_r < 80°$. Clearly a full quantum calculation would generate the correct intensities, but because of the large number of scattering channels ($> 10^3$) it would involve massive computer time. A three-dimensional semiclassical calculation using classical-trajectory Monte Carlo methods is a tractable computation even for a unit mesh containing 49 atoms.[6] One may assume in analogy with He scattering from other surfaces (alkali halides, platinum silicide) an attractive well perhaps 10–20 meV in magnitude. This well is expected to have a noticeable refraction effect on some of the angular profiles and will have to be taken into account in a structural calculation. For example, in Fig. 3, $\theta_i = 30°$, there is a distinct alternating sequence of peaks extending from $\Delta K_{\parallel} = -1.0$ to 0. At $\theta_i = 45°$ this sequence has apparently shifted to $\Delta K_{\parallel} = +0.6$, a change in θ_r of 30°, although hard-wall scattering would predict a change of only 15° in θ_r.

In conclusion, we have presented a set of atomic diffraction spectra for He scattering from the Si(111) surface which show the outermost exposed layer to be reconstructed into a 7×7 unit mesh as expected from previous LEED studies. In contrast to LEED, however, these diffraction intensities are determined by scattering only from the top double layer. A large number of diffraction peaks are observed in each spectrum for a range of incident angle and two wavelengths. The total diffraction intensity in plane is of the order of $\frac{1}{2}\%$ of the incident beam. Strong vicinal out-of-plane peaks recorded in scans using a larger detector acceptance angle (1.4°) indicate that the total diffractive scattering may be a substantial fraction of I_0 as expected for an estimated surface Debye temperature of 360 K.[5] There is some indication that a hard-wall potential with a weak attractive well is appropriate for this scattering system. The different structural models which have been proposed for the Si(111) 7×7 reconstruction[7-9] are expected to generate quite different intensity sequences versus θ_r for the range of incident conditions we report. Consequently, we think that the data we present here are sufficient to give each model a critical test.

[1]R. E. Schlier and H. E. Farnsworth, J. Chem. Phys. 30, 917 (1959); J. J. Lander and J. Morrison, J. Chem. Phys. 37, 729 (1962).

[2]Cf. W. Mönch and P. P. Auer, J. Vac. Sci. Technol. 15, 1230 (1978), and references therein.

[3]M. J. Cardillo, C. C. Ching, E. F. Greene, and G. E. Becker, J. Vac. Sci. Technol. 15, 423 (1978).

[4]M. J. Cardillo and G. E. Becker, Phys. Rev. Lett. 40, 1148 (1978).

[5]Assuming $\theta_D^{\text{surface}} = \frac{2}{3}\theta_D^{\text{bulk}}$, with $\theta_D^{\text{bulk}} = 543$ K [B. W. Batterman and D. R. Chipman, Phys. Rev. 127, 690 (1962)], we estimate a reduction in the total diffraction intensities to $I/I_0 = 10-20\%$, for a range of the He/Si attractive well depth of 10–20 meV.

[6]E. Grimmelmann and J. C. Tully, private communication.

[7]J. J. Lander and J. Morrison, J. Appl. Phys. 34, 1403 (1963).

[8]W. A. Harrison, Surf. Sci. 55, 1 (1976).

[9]J. D. Levine, S. H. McFarlane, and P. Mark, Phys. Rev. B 16, 5415 (1977).

Sample-Shape-Dependent Phase Transition of Hydrogen in Niobium

H. Zabel

Sektion Physik der Universität München, D 8000 München 22, Germany, and Department of Physics, University of Houston, Houston, Texas 77004[(a)]

and

H. Peisl

Sektion Physik der Universität München, D 8000 München 22, Germany

(Received 13 December 1978)

The coherent α-α' phase transiton of H in Nb has been studied in several sample shapes. The samples were loaded *in situ* with the critical hydrogen concentration of 0.31 H/Nb above $T_c = 171$°C and slowly cooled. Below T_c a coherent macroscopic spinodal decomposition takes place. By x-ray scattering and examination of the relaxed crystals, the spatial arrangement of the phases was determined. The macroscopic modes so revealed depend sensitively upon sample shape through the fulfillment of the elastic boundary condition.

The α-α' phase transition of H in Nb resembles a gas-liquid transition of a real gas.[1,2] In this transition the lattice retains its original bcc symmetry, and the phases are only distinguishable by their different lattice expansions. This transition and similar transitions in PdH (Ref. 3) and PdAgH (Ref. 4) are still under discussion.[5,6] They have often been treated as textbook examples of a lattice gas,[7,8] and the interaction energy, responsible for the phase transition, is introduced as a suitable parameter proportional to the measured critical temperature T_c. In contrast to the lattice-gas model the real lattice is deformable and the interstitially dissolved protons set up long-range distortion fields.[9-11] The α-α' transition has therefore been attributed to an elastic interaction via this lattice distortion induced by the protons.[12,13] The model of elastic interaction leads in turn to the concept of macroscopic elastic modes[14,15] caused by internal stress produced by the inhomogeneous hydrogen density variation in a coherent lattice. At T_c only a few modes become unstable which depend upon the sample geometry through the fulfillment of the elastic boundary condition. Therefore, the study of the shape dependence of the phase transition is a crucial test of the validity of the elastic interaction as the main contribution to the attractive part of the energy.

Nb samples (single crystals, wires, and foils)

